# Modulation frequency response of a bistable system with noise

Bob Nagler,* Guy Verschaffelt, Michael Peeters, Jan Albert, Irina Veretennicoff, and Jan Danckaert
*Department of Applied Physics and Photonics (TW-TONA), Vrije Universiteit Brussel, Pleinlaan 2, B-1050 Brussels, Belgium*

Giovanni Giacomelli
*Instituto Nazionale di Ottica Applicata (INOA), Largo E. Fermi 6, 50125 Firenze, Italy and INFM, Unità di Firenze, Firenze, Italy*

Francesco Marin
*INFM, Unità di Firenze and Dipartimento di Fisica and LENS, Università di Firenze, via Sansone 1, 50019 Sesto Fiorentino, Italy*
(Received 25 May 2004; published 25 October 2004)

We present a method to construct a modulation frequency response curve for bistable systems in the presence of noise. To this end, a small sinusoidal modulation is applied to the system such that it switches between its two stable states. The response curve we construct yields information on the nature of the physical mechanism underlying the switching process and is furthermore comparable to the standard response curves of linear systems. Our semianalytical approach, which only needs approximate Kramer rates, is in good agreement with numerical simulations. The concept is applicable to a wide range of systems.

DOI: 10.1103/PhysRevE.70.046214 PACS number(s): 05.45.−a, 43.50.+y, 42.60.Mi, 42.65.Sf

## I. INTRODUCTION

Since the introduction of stochastic resonance (see Gammaitoni *et al.* [1] for an overview) in the 1980s, there has been a renewed interest in the effect of small noise on the response of modulated systems. Stochastic resonance has since been studied in the adiabatic and in the linear response limit [2–5] and beyond [6,7]. It has been experimentally observed in many systems of a very diverse nature [8–12].

In this paper we tackle a related topic and study the frequency response of a bistable system with noise. We developed this frequency response in such a way that it can be compared directly with standard frequency responses of linear systems. In a linear system one usually determines the transfer function of the system using an input signal with constant amplitude and recording the output amplitude at different input frequencies. In a noisy bistable system, this is no longer possible as the output hops stochastically between two states and hence the output amplitude is fixed by the distance between the two stable points. We propose to record the minimum input amplitude necessary to achieve a certain error rate in the output signal. The inverse of this minimum amplitude leads to an alternative definition of the modulation frequency response. This stochastic frequency response (SFR) is a tool to study the physical effects causing the bistability and switching between the two stable states, much as the frequency response of a linear system yields information about the studied system. Furthermore, using the transition rates between the stable states, we can derive a semianalytical formula for this SFR and obtain a closed form for the asymptotic behavior near the stochastic resonance peak in the SFR.

In Sec. II we introduce the general idea and the method used to record the frequency response of a bistable system. Section III is devoted to the theoretical study of the SFR and culminates in an analytical expression. Our results can be applied to any bistable system. As a first example, we apply it in Sec. IV A to a bistable system with Kramers transition rates proposed by McNamara and Wiesenfeld [2]. A more applied result is given in Sec. IV B, where we use it to determine the influence of a limiting time scale on polarization switching in vertical-cavity surface-emitting lasers (VCSEL's). A summary of the most important findings concludes this paper in Sec. V.

## II. DEFINITION OF THE STOCHASTIC FREQUENCY RESPONSE

Consider the following one-dimensional Langevin equation (see Refs. [1,2]):

$$\dot{x} = \frac{-dV(x)}{dx} + \sqrt{2D}\tilde{\xi}(t), \tag{1}$$

with the potential $V(x)$ given by

$$V(x) = -\frac{1}{2}x^2 + \frac{1}{4}x^4 + Jx, \tag{2}$$

with $\delta$-correlated noise

$$\langle \tilde{\xi}(t)\tilde{\xi}(s)\rangle = \delta(t-s), \tag{3}$$

and $J$ a parameter that can be modulated. The potential for $J=0$ is plotted in Fig. 1. It has a stable state at +1 and one at −1 (from now on called the "+" mode and the "−" mode). Due to the noise, spontaneous transitions between the stable

*Current address: Lawrence Berkeley National Laboratory, Center for Beam Physics, LBNL, 1 Cyclotron Rd., Berkeley, CA 94720, USA. Electronic address: Bob.Nagler@fulbrightweb.org; URL: http://www.tona.vub.ac.be

 

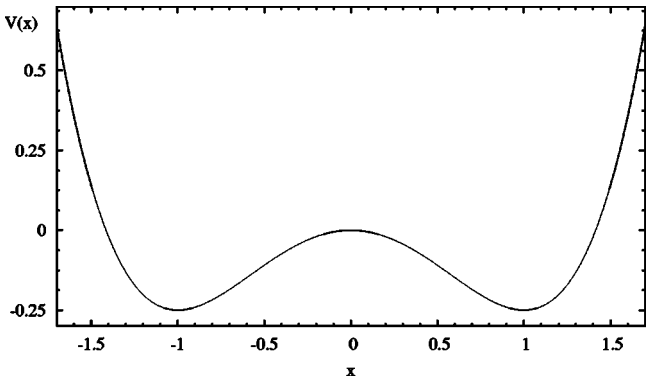


FIG. 1. Potential as given by Eq. (2) for $J=0$. Two stable states can be found at $x=+1$ and $x=-1$.

states occur. When the parameter $J$ is modulated with an amplitude $J_m$ around a bias point $J_b$ at pulsation $\omega$ such that

$$J = J_b + J_m \sin(\omega t + \phi), \tag{4}$$

switching between the two stable states is observed. We explicitly introduce an initial phase $\phi$ because we will later define $t=0$ as the time corresponding to a switching event (see Sec. III). Depending on the frequency and amplitude, the system will follow the modulation. Stochastic resonance occurs (for small amplitudes in the adiabatic limit) when the frequency of the modulated signal equals one-half of the Kramers escape rate $r_K$ (see Refs. [1,2]). A typical time trace of $x$ when $J$ is modulated according to Eq. (4) can be seen in Fig. 2.

It is obvious that stochastic effects play an important role: the switching between the two stable modes occurs with a random delay when we modulate $J$. If this delay is longer than half a modulation period, a switch will be missed. We define here a *successful* modulation cycle as one where the system switches up and down during one modulation period. From the time trace of $x$ we can deduce the fraction of such successful cycles. As we have to determine the percentage of successful switches for a large number ($\sim$100 000) of modulation cycles to obtain statistically relevant data, we will actually count the number of missed switches by looking at the histogram of the time the system stays in one mode before jumping to the other one. The histograms of these residence times $[P_r(t)]$ of both stable modes can be seen in Fig. 3.

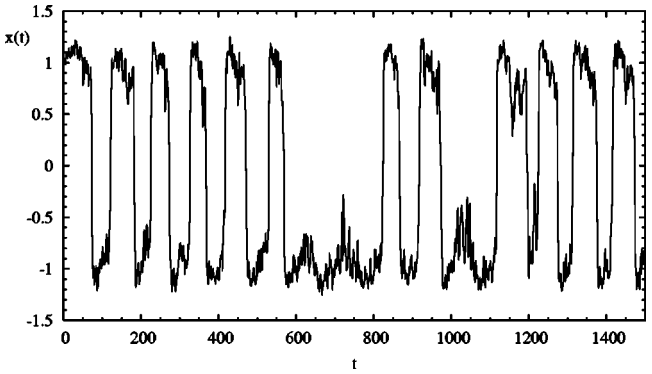


FIG. 2. Time traces of $x$, obtained by numerically solving Eq. (1). Parameter values are $D=0.048$, $T=2\pi/\omega=100$, $J_b=0$, and $J_m=0.31$.

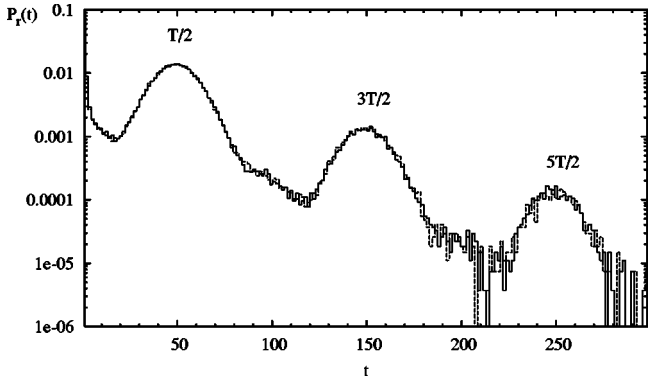


FIG. 3. Numerical histograms of the residence times $P_r(t)$ in the "+" mode (solid line) and in the "−" mode (dashed line). Derived from a time trace of 100 000 modulation periods. Same parameter values as in Fig. 2.

Consider the "+" mode in Fig. 2. The residence time of this mode is nearly always close to $T/2$. Therefore the histogram, or probability density function, of the residence time has a peak at $T/2$. The peak is rather broad, since there is some spread in the value of the residence time. If the system does not switch around $T/2$, it will often stay in the "+" mode for one and a half periods, having another chance to switch in the next modulation cycle. There is one such occurrence in Fig. 2. These events cause the second peak (around $3T/2$) in the histogram in Fig. 3. The third-, fourth-, and higher-order peaks are caused when the system misses its cue twice, thrice, four times, etc. The same story applies to the residence time of the "−" mode.

In Fig. 3 the height of each peak is a fraction $F$ of that of the previous peak. In Sec. III we show that this fraction is the same for any two consecutive peaks and that the shape of the peaks remains the same. The magnitude $F$ of this decrease actually depends on the modulation amplitude, which we chose such to have a decrease between consecutive peaks of one decade. If we call $P_r(t)$ the probability density function of the residence times, a decrease of one decade implies that

$$\log_{10} P_r(t+T) = \log_{10} P_r(t) - 1 \tag{5}$$

or

$$P_r(t+T) = \frac{1}{F} P_r(t) = \frac{1}{10} P_r(t). \tag{6}$$

A successful switch is in principle defined by integrating $P_r(t)$ over a modulation period $T$ around the position of the first peak. However, such an indicator is too sensitive to the background (i.e., the switches that take place in the absence of an input modulation signal) [13]. To avoid this problem, we integrate $P_r(t)$ over a $T/2$ width and we will only work at frequencies above the stochastic resonance frequency. After integration of $P_r(t)$ over half a modulation period $T/2$ around the position of the first peak, we obtain the probability of a successful up switch (i.e., a switch from the "−" to the "+" mode), whereas such an integration around the position of

the second peak yields the probability of a switch being missed once. Because the shape of the different peaks in Fig. 3 is the same, the integral of $P_r(t)$ will scale in the same way over a modulation period as the height of the peaks. Therefore, the probability of a successful up switch is 10 times larger than the probability a switch is missed once, which is in its turn 10 times larger than the probability a switch is missed twice, and so forth. So a one decade difference means that 90% of the up switches are successful, as

$$\left(1-\frac{1}{F}\right)\sum_{n=0}^{\infty}\left(\frac{1}{F}\right)^n = 0.9 + 0.09 + 0.009 + \cdots = 1. \quad (7)$$

Similarly, 90% of the down switches (i.e., switches from the "+" to the "−" mode) are successful. For a successful cycle, both the up and down switches need to happen, leading to a probability of a successful cycle of 81% for the situation depicted in Fig. 3.

We now define the *stochastic frequency response as the inverse of the modulation amplitude needed to have a fixed level of successful cycles as a function of the modulation frequency*. We use in this definition a fixed level of 81%. In principle, one can choose a higher percentage, but this will considerably lengthen the measurement (or integration) time as in that case a missed switch only happens sporadically and enough missed switches are needed to obtain a statistically relevant histogram.

As we will show, to compare the SFR with standard responses of linear systems we need to look at the inverse of the modulation amplitude. Indeed, in linear systems, the response to a harmonic modulation is given by

$$O(\omega) = H(\omega)I(\omega), \quad (8)$$

where $I(\omega)$ is the Fourier transform of the input variable and $O(\omega)$ is the Fourier transform of the output variable. A standard procedure to determine the transfer function $H(\omega)$ is to take a monochromatic input $I(\omega)$ with constant amplitude and measure the output $O(\omega)$ as a function of the modulation frequency. $O(\omega)$ then equals the transfer function.

However, this is not possible for bistable systems in which an input signal $I(\omega)$ at frequency $\omega$ does not give in general a periodic output, as is evident from the time trace shown in Fig. 2. The problem that we want to address is how to characterize quantitatively the response of a bistable system, such that it sheds light on the physical phenomena regulating its dynamics. In our picture, the input variable [in Eq. (2) the parameter $J$] drives an intermediate variable $O_1(\omega)$ through linear mechanisms. $O_1(\omega)$ is the origin of the bistability and drives the switching process, but is not directly accessible. Our aim is to obtain the response function linking $O_1(\omega)$ to the input variable, thus getting useful information about the underlying physics. For this purpose, we invert the problem and introduce a suitable indicator $f(O_2(\omega))$ based on the output $O_2(\omega)$ of the system: the percentage of successful modulation cycles. We assume that if the number of successful switches is the same for different frequencies or

$$f(O_2(\omega_1)) = f(O_2(\omega_2)), \quad (9)$$

then the output variable $O_1(\omega)$ we want to characterize is also the same or

$$O_1(\omega_1) = O_1(\omega_2). \quad (10)$$

If we use a monochromatic input signal and change its amplitude in order to have a fixed $f(O_2(\omega))$, we can say that

$$O_1(\omega) = H(\omega)I(\omega) = \text{const}, \quad (11)$$

similarly as in Eq. (8). So finally we obtain the frequency response of our bistable system by inverting the previous equation:

$$H(\omega) = \frac{\text{const}}{I(\omega)}. \quad (12)$$

This is why we use in our definition of the SFR the *inverse* of the modulation amplitude needed to get 81% successful cycles.

The above treatment can only be performed for frequencies above the stochastic resonance frequency. At lower frequencies, the histograms lose their distinct peaks at odd multiples of half the modulation period and tend towards a single peak on an exponential background. Our definition of the SFR cannot be used in this case, because it can only be applied with at least two peaks in the histogram.

We will now show how such a stochastic frequency response is fully determined by the transition rates of the two stable modes.

## III. THEORETICAL TREATMENT

If the parameter $J$ in Eq. (1) is not equal to zero, the potential is skewed and the transition rates $r_+$ and $r_-$ of the two states are no longer equal. If moreover the parameter $J$ depends on time, the transition rates $r_\pm$ will also be modulated in time. The rates $r_\pm$ can, in principle, be derived from the Langevin equation of the system, although in practice this is usually too difficult to do analytically. But anyway, the histograms of the residence times $P_{m_\pm}(t)$ are given by (see Ref. [1])

$$P_{m_\pm}(t) = r_\pm(J)\exp\left[-\int_0^t r_\pm(J)dt\right]. \quad (13)$$

The time dependence in Eq. (13) stems from the fact that we are modulating the parameter $J$ according to Eq. (4). One has to be careful, however, that the distribution of Eq. (13) is not the distribution of the measured residence times plotted in Fig. 3; it is the distribution of the time the system stays in the "+" mode ("−" mode) if it was in that mode at time $t=0$. So it is only the residence time of the "+" mode ("−" mode), when the system switched to that mode at time $t=0$ or, in other words, for a fixed phase relation between the input modulation and the switch. To get the distribution of the phase independent residence time, we have to average over all possible phases (we write the dependence of $P_{m_\pm}$ on $\phi$ explicitly):

$$P_{r_\pm}(t) = \int P_{m_\pm}(t,\phi)P_{\pm\phi}(\phi)d\phi, \tag{14}$$

where $P_{\pm\phi}(\phi)$ is the probability density that the system switched to the "+" mode ("−" mode) with a phase $\phi$ with respect to the modulation. Unfortunately, there is no known method to derive this phase distribution $P_{\pm\phi}$, although in some limits self-consistent distributions have been proposed in the literature (see Refs. [1,3–5]).

Even without knowing the expression for Eq. (14), we can get the information we need to derive an expression for the SFR. Indeed, this frequency response is derived from the modulation amplitude which leads to 81% successful cycles or a difference of one decade between consecutive peaks in the residence time distribution. Therefore, we only need the relation between the height of consecutive peaks. We will derive an expression for $P_{r_\pm}(t+T)$, with $T$ being the period of modulation. We write

$$P_{m_\pm}(t,\phi) = r_\pm(t,\phi)\exp[G_\pm(t,\phi)], \tag{15}$$

defining

$$G_\pm(t,\phi) = -\int_0^t r_\pm(t,\phi)dt. \tag{16}$$

We have

$$r_\pm(t+T,\phi) = r_\pm(t,\phi), \tag{17}$$

as $r_\pm$ is periodic, and

$$G_\pm(t+T,\phi) = -\int_0^{t+T} r_\pm(t,\phi)dt$$

$$= -\int_0^T r_\pm(t,\phi)dt - \int_T^{T+t} r_\pm(t,\phi)dt \tag{18}$$

$$= G_\pm(T,\phi) - \int_0^t r_\pm(t,\phi)dt \tag{19}$$

$$= G_\pm(T) + G_\pm(t,\phi). \tag{20}$$

Note that $G_\pm(T)$ is independent of the phase

$$G_\pm(T) = G_\pm(T,\phi)\ \forall\ \ \phi, \tag{21}$$

since it is the integral of a periodic function over one period. So we have

$$P_{m_\pm}(t+T,\phi) = P_{m_\pm}(t,\phi)\exp[G_\pm(T)]. \tag{22}$$

Substituting in Eq. (14) yields

$$P_{r_\pm}(t+T) = \exp[G_\pm(T)]P_{r_\pm}(t). \tag{23}$$

A decrease of the height with a factor $F=e^d$ between consecutive peaks of $P_{r_\pm}$ is attained if

$$d = \ln[P_{r_\pm}(t)] - \ln[P_{r_\pm}(t+T)] = -G_\pm(T) \tag{24}$$

$$= \int_0^T r_\pm(t,\phi)dt. \tag{25}$$

The phase $\phi$ in this equation is irrelevant as explained by Eq. (21) and can therefore be left out. We fix $d=\ln(10)$ as a reference value, which corresponds to a decrease of one decade. So we have to solve

$$\ln(10) = \int_0^{2\pi/\omega} r_\pm(J_b + J_m\sin\omega t)dt. \tag{26}$$

We remark that Eq. (26) represents two equations: one for $r_-$ and one for $r_+$. Therefore we have two integral equations to solve for two variables $J_b$ and $J_m$. Plotting the inverse of $J_m$ as a function of frequency gives the stochastic frequency response curve, as explained in Sec. II. Equation (26) is one of the main theoretical results of this paper. It allows us to generally evaluate the frequency response of a bistable system and compare it with standard linear systems theory. To show its validity and uses, we will apply it in the next section to two problems: a simple bistable system with escape rates proposed by McNamara and Wiesenfeld (see Ref. [2]) and the problem of determining the influence of a limiting time scale on polarization switching in VCSEL's.

## IV. APPLICATIONS

### A. Frequency response of a simple bistable system

To study the general traits of the frequency response curve we start with the modulated escape rates proposed by McNamara and Wiesenfeld [2] with the bias $J_b$ of the modulation fixed at 0:

$$r_\pm(t) = r_K\exp\left[\pm\frac{J_m}{D}\cos(\omega t)\right], \tag{27}$$

where the Kramer transition rate $r_K$ (see Refs. [14,15]) is given by

$$r_K = \frac{1}{\sqrt{2\pi}}e^{-1/4D}. \tag{28}$$

As in Refs. [1,2] we assume that the modulation amplitude is small, so we can develop Eq. (27) as follows:

$$r_\pm(t) \simeq r_K\left[1 \pm \frac{J_m}{D}\cos(\omega t) + \frac{1}{2}\left(\frac{J_m}{D}\right)^2\cos^2(\omega t)\right]. \tag{29}$$

We actually take Eq. (29) as a starting point of the analysis and calculate the corresponding frequency response.[1] We now combine Eqs. (25) and (29). The frequency response which we defined in Sec. II [Eq. (12)] to be the inverse of the modulation amplitude then equals

[1] In fact we also look at the modulation regions where Eq. (29) is not a good approximation of Eq. (27).

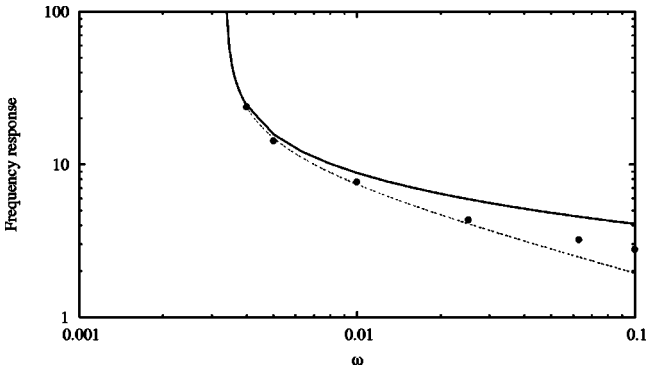


FIG. 4. SFR obtained from simulations of Eqs. (1)–(3) (circles), semianalytical calculations using Eq. (26), and escape rates given by Eq. (27) (solid line) and plot of $H(\omega)$ [Eq. (30)] (dashed line). Parameter values used are $d=\ln(10)$ and $D=0.048$, which correspond to a stochastic resonant pulsation of $\omega_{\mathrm{SR}}=3.87\times10^{-3}$. The asymptote near the stochastic resonance peak is clearly visible.

$$H(\omega)=\left(D\sqrt{\frac{2(d\omega-2\pi r_K)}{\pi r_K}}\right)^{-1}. \tag{30}$$

Equation (30) is plotted in Fig. 4 together with the frequency response as obtained from simulations of Eqs. (1)–(3) and semianalytical calculations using Eqs. (26) and (27). The stochastic effects clearly cause a slope in the frequency response, which flattens for high frequencies. There is a good correspondence between simulations, the semianalytical frequency response calculated by numerically solving Eq. (26), and the full analytical approach [Eq. (30)]. At higher frequencies, Eq. (30) deviates from the simulations because the approximation in Eq. (29) is only valid for small modulation amplitudes. The differences between the simulations and the semianalytical calculations are caused by the limited validity of the escape rates: Eq. (27) is also only valid for small modulation amplitudes.

The asymptote in Fig. 4 at $\omega=3.36\times10^{-3}$ is due to the phenomenon of stochastic resonance. Its place is, however, also determined by the value of $d$ [the exponential decrease of the peaks in the residence time distribution—see Eq. (24)]: indeed we have

$$\omega_\infty=\frac{2\pi r_K}{d}=\frac{2}{d}\omega_{\mathrm{SR}}, \tag{31}$$

where $\omega_{\mathrm{SR}}=\pi r_K$ is the modulation frequency for which stochastic resonance occurs (see Refs. [1,2]). For the parameter values used in Fig. 4 this results in $\omega_\infty=0.003\,36$. This value corresponds exactly to the position of the asymptote in Fig. 4. Note that Eq. (31) is not only valid for switching rates given by Eq. (29), but also for Eq. (27) and for more general well-behaving rates, since the approximation $J/D\ll1$ is valid at the asymptote, where the modulation amplitude vanishes.

### B. Frequency response of polarization switching in VCSEL's

We will now study the stochastic frequency response of polarization switching in vertical-cavity surface-emitting lasers. This will not only show us a real-world example of such a stochastic frequency response, but we will also demonstrate how this method can be used to determine the physical mechanism causing the switching and hence the bistability in the system. VCSEL's are semiconductor lasers that emit light in a single longitudinal mode perpendicular to the substrate on which they are fabricated. In their single-transverse-mode regime, they usually emit linearly polarized light in one of two orthogonal linear polarization modes. In some VCSEL's, abrupt polarization switching (PS) between these polarization modes (PM's) is observed when the injected current is changed. To model this PS we will use a phenomenological intensity rate-equation model introduced in Refs. [16,17], which has been shown to adequately describe the VCSEL's polarization response. The key ingredients in our intensity rate-equation model are (i) current- or temperature-dependent gain coefficients for the two polarization modes, which cause PS to occur at the current or temperature where the gains equalize, and (ii) gain saturation coefficients, which induce a region of bistability around the switching point. Furthermore, in this model time is reduced with respect to the carrier lifetime. The carrier noise is neglected; as in VCSEL's, it is much smaller than the spontaneous emission noise. Written down in dimensionless parameters these equations are [16,17]

$$\frac{dp_x}{dt}=p_x\left[\eta-\varepsilon_s p_x-\varepsilon_c p_y-\frac{G}{2}\right]+\frac{1}{2}R_{sp}+\tilde{F}_x,$$

$$\frac{dp_y}{dt}=p_y\left[\eta-\varepsilon_s p_y-\varepsilon_c p_x+\frac{G}{2}\right]+\frac{1}{2}R_{sp}+\tilde{F}_y,$$

$$\frac{d\eta}{dt}=\frac{J-p_x-p_y}{\rho}-\eta-p_x[\eta-\varepsilon_s p_x-\varepsilon_c p_y]-p_y[\eta-\varepsilon_s p_y-\varepsilon_c p_x], \tag{32}$$

where $p_{x,y}$ are the photon densities in the two PM's, $\varepsilon_{s,c}$ are the optical saturation coefficients, $\eta$ is the deviation of the carrier density from its threshold value, $G$ is the gain difference between the PM's, and $J$ is the dimensionless current above threshold given by $J=(I-I_{th})/I_{th}$ with $I$ being the current (in mA) and $I_{th}$ being the VCSEL's threshold current (in mA). $R_{sp}$ is the mean power spontaneously emitted in the PM's, $\rho$ is the ratio of the photon to the carrier lifetime, $t$ is the reduced time, and $\tilde{F}_{x,y}$ are stochastic terms describing the spontaneous emission noise with correlation functions

$$\langle\tilde{F}_{x,y}(t)\tilde{F}_{x,y}(s)\rangle=2\,R_{sp}p_{x,y}\delta(t-s). \tag{33}$$

The stochastic differential equations (32) have to be interpreted in the Stratonovich sense [18]. The $p_x$ ($p_y$) mode plays the role of the "−" ("+") mode of Sec. III. Finally, the polarization switching is induced by changes in the gain difference $G$ when the injected current $J$ is changed, which we express as

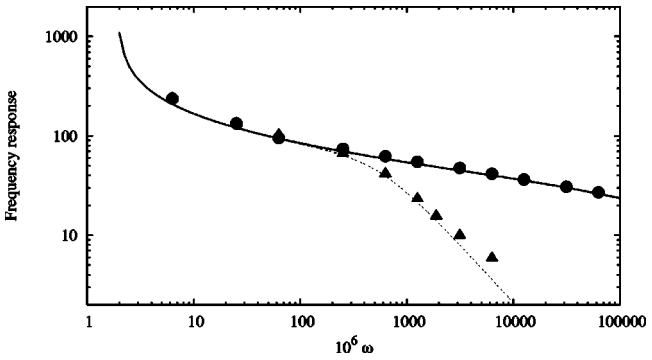


FIG. 5. Polarization switching frequency response simulated using Eqs. (32)–(34) (circles) and semianalytically calculated using Eqs. (26) and (35) (solid line). Also shown are the simulated (triangles) and semianalytical (dashed line) frequency responses if a slow time scale as in Eqs. (38) and (39) is taken into account. The parameter values used are $J_{switch}=0.4$, $\epsilon_c-\epsilon_s=8.47$, $R_{sp}=0.022$, $\rho=0.001$, $g=25.3$, and $\rho_\Gamma=1770$ and correspond to a real device [19].

$$G = g\left(1 - \frac{J}{J_{switch}}\right), \tag{34}$$

where $J_{switch}$ is the current at which the PS happens and $g$ specifies the magnitude of the gain difference. After reduction of Eqs. (32) to a one-dimensional Langevin equation describing the intensity in one of the polarization modes, we can obtain the transition rates $r_\pm$ between the two polarization modes (see Ref. [17]):

$$\frac{1}{r_\pm} = \frac{2\pi J\delta\epsilon}{(-G + J\delta\epsilon)(G + J\delta\epsilon)}\mathrm{erf}\left[\frac{(G \pm J\delta\epsilon)}{2\sqrt{R_{sp}\delta\epsilon}}\right]\mathrm{erfi}\left[\frac{(G \pm J\delta\epsilon)}{2\sqrt{R_{sp}\delta\epsilon}}\right], \tag{35}$$

where $\delta\epsilon=\varepsilon_c-\varepsilon_s$, erf is the error function, and erfi is the imaginary error function. Using these transition rates, we can calculate the frequency response from Eq. (26). This is shown in Fig. 5 (circles) and compared with simulations of the frequency response based on the full set of equations (32) (solid line). The excellent agreement between simulations and semianalytical calculations confirms the validity of Eq. (26). The asymptote in Fig. 5 at $\omega=1.9\times10^6$ is due to stochastic resonance and agrees well with the calculated value $\omega=1.89\times10^6$ of this asymptote using Eq. (31).

This frequency response can be used to determine the physical mechanism of the switching (and consequently of the bistable system). Indeed, consider that the parameter $J$ which is experimentally available (and is modulated) does not directly influence the potential of the system, but does so through a linear system $H_1(\omega)$. If we call $\Gamma$ the parameter that determines the potential, then we have

$$\Gamma(\omega) = H_1(\omega)J(\omega). \tag{36}$$

The total response curve of the system is still given by the inverse of the needed amplitude of $J$:

$$H_{\mathrm{tot}}(\omega) = H_1(\omega)\Gamma^{-1}(\omega) = H_1(\omega)H_{\mathrm{fr}}(\omega). \tag{37}$$

The total response curve is simply the product of the direct frequency response $H_{\mathrm{fr}}$ and $H_1$. In other words we can work with such a definition of the frequency response in bistable systems as if we were dealing with linear response curves. This way, $H_1$ (i.e., the physical mechanism that links the modulated parameter with the change in potential) can be identified.

As an example of this technique, let us consider that the gain difference $G$ between the polarization modes in our VCSEL is not directly influenced by the injected current, but through another parameter $\Gamma$ which in its turn depends on the injected current. We assume that $\Gamma$ only reacts to current fluctuations through a linear first-order response with a slow time constant such that

$$G = g\left(1 - \frac{\Gamma}{J_{switch}}\right) \tag{38}$$

and

$$\frac{d\Gamma}{dt} = \frac{J - \Gamma}{\rho_\Gamma}, \tag{39}$$

where $\rho_\Gamma$ is the ratio of $\Gamma$'s time constant to the carrier lifetime. The resulting frequency response is also shown in Fig. 5. Again there is good correspondence between the simulations and semianalytical calculations. Moreover, the frequency response calculated using Eq. (38) matches very well with the response that one would obtain by multiplying the response calculated according to Eq. (34) with a first-order transfer function (not shown) as indicated by Eq. (37). In this frequency response we can clearly see the effect of the slow time scale at which $\Gamma$ reacts. If one measures such a frequency response for a particular device, the time scale—which is intimately linked with the underlying physical process—that determines the switching can be easily identified. This method can, for instance, be used to study the influence of thermal effects on the PS in a VCSEL. Thermal effects typically happen with a slow time constant (about 10 μs) and can be directly measured by looking at the temperature-dependent frequency shift of the emitted light (or chirp). In Refs. [19,20] such a comparison between the measured thermal and PS frequency response was successfully used to show that PS in some VCSEL's is (at least partially) due to thermal effects.

## V. CONCLUSION

In this paper we presented a method to determine a frequency response curve in a bistable system with noise. This SFR can be compared with classical responses of linear systems. It is defined as the inverse of the modulated amplitude that is needed to get a fixed value of successful switches between the two stable states of the system under test. The definition is only valid for frequencies above the stochastic resonance frequency, whereas the asymptote in the frequency response curve clearly shows the presence of stochastic resonance.

We have derived an equation to calculate this frequency response based solely on the transition rates between the two stable states of the system. The validity of this equation was checked on two example bistable systems.

Moreover, we have shown how this method can be used to characterize the underlying physical mechanism of the switching (and consequently of the bistable system). If the parameter that influences the potential of the system is not directly experimentally available, we can still see its impact on the frequency response. The total response curve is in that case simply the product of the direct frequency response and the frequency response of the parameter determining the potential. This technique was experimentally used in Refs. [19,20] to identify the physical mechanism causing polarization switching in particular VCSEL's.

## ACKNOWLEDGMENTS

This research was supported by the Belgian Interuniversity Attraction Pole Program (IAP V-18), the Concerted Research Action "Photonics in Computing," the research council (OZR) of the VUB, and EU RTN network VISTA (Contract No. HPRN-CT-2000-00034). B.N., G.V., and J.D. acknowledge the Fund for Scientific Research, Flanders (FWO) for their financial support.

[1] L. Gammaitoni, P. Hänggi, P. Jung, and F. Marchesoni, Rev. Mod. Phys. **70**, 223 (1998).
[2] B. McNamara and K. Wiesenfeld, Phys. Rev. A **39**, 4854 (1989).
[3] R. Löfstedt and S. N. Coppersmith, Phys. Rev. Lett. **72**, 1947 (1994).
[4] R. Löfstedt and S. N. Coppersmith, Phys. Rev. E **49**, 4821 (1994).
[5] M. H. Choi, R. F. Fox, and P. Jung, Phys. Rev. E **57**, 6335 (1998).
[6] P. Jung and P. Hänggi, Europhys. Lett. **8**, 505 (1989).
[7] P. Jung and P. Hänggi, Phys. Rev. A **44**, 8032 (1991).
[8] I. Claes and C. Van den Broeck, Phys. Rev. A **44**, 4970 (1991).
[9] J. K. Douglass, L. Wilkens, E. Pantazelou, and F. Moss, Nature (London) **365**, 337 (1993).
[10] K. Wiesenfeld and F. Jaramillo, Chaos **8**, 539 (1998).
[11] P. Hänggi, ChemPhysChem **3**, 285 (2002).
[12] B. Nagler, M. Peeters, I. Veretennicoff, and J. Danckaert, Phys. Rev. E **67**, 056112 (2003).
[13] S. Barbay, G. Giacomelli, and F. Marin, Phys. Rev. E **61**, 157 (2000).
[14] H. A. Kramers, Physica (Amsterdam) **7**, 284 (1940).
[15] P. Hänggi, P. Talkner, and M. Borkovec, Rev. Mod. Phys. **62**, 251 (1990).
[16] J. Danckaert, B. Nagler, J. Albert, K. Panajotov, I. Veretennicoff, and T. Erneux, Opt. Commun. **201**, 129 (2002).
[17] B. Nagler *et al.*, Phys. Rev. A **68**, 013813 (2003).
[18] H. Risken, *The Fokker-Planck Equation* (Springer-Verlag, Berlin, 1996).
[19] G. Verschaffelt, J. Albert, B. Nagler, M. Peeters, J. Danckaert, S. Barbay, G. Giacomelli, and F. Marin, IEEE J. Quantum Electron. **39**, 1177 (2003).
[20] G. Verschaffelt, J. Albert, I. Veretennicoff, J. Danckaert, S. Barbay, G. Giacomelli, and F. Marin, Appl. Phys. Lett. **80**, 2248 (2002).